Reinitiation after Translation of Two Upstream Open Reading Frames (ORF) Governs Expression of the ORF35-37 Kaposi's Sarcoma-Associated Herpesvirus Polycistronic mRNA

Lisa M. Kronstad,[a] Kevin F. Brulois,[b] Jae U. Jung,[b] Britt A. Glaunsinger[a]

Department of Plant and Microbial Biology, University of California, Berkeley, California, USA[a]; Department of Molecular Microbiology and Immunology, Keck School of Medicine, University of Southern California, Los Angeles, California, USA[b]

The Kaposi's sarcoma-associated herpesvirus (KSHV) ORF36 protein kinase is translated as a downstream gene from the ORF35-37 polycistronic mRNA via a unique mechanism involving short upstream open reading frames (uORFs) located in the 5′ untranslated region. Here, we confirm that ORF35-37 is functionally dicistronic during infection and demonstrate that mutation of the dominant uORF restricts KSHV replication. Leaky scanning past the uORFs facilitates ORF35 expression, while a reinitiation mechanism after translation of the uORFs enables ORF36 expression.

Similarly to other double-stranded DNA (dsDNA) viruses, the vast majority of Kaposi's sarcoma-associated herpesvirus (KSHV) gene expression conforms to the eukaryotic paradigm of cap-dependent translation of a single protein per mRNA. The sole viral protein expressed exclusively from a functionally polycistronic mRNA is the ORF36 protein kinase, a viral factor that activates the c-Jun N-terminal kinase (JNK) signaling pathway and sensitizes KSHV-infected cells to ganciclovir (1–6). The viral ORF35-37 polycistronic mRNA directs synthesis of both ORF35 and ORF36, whereas ORF37 is translated from an independent monocistronic transcript (7). A key mechanism underlying the dicistronic character of the ORF35-37 mRNA involves reinitiation after translation of an out-of-frame short upstream open reading frame (uORF2) that overlaps with ORF35 (Fig. 1A to C) (7). Short uORFs are common regulatory elements in mammalian transcripts that generally function to dampen translation of the major ORF by capturing a population of the scanning ribosomes (8). They are prevalent in several viruses as well, and those that have been characterized appear to function in an analogous manner (9–11). However, KSHV has adopted this cellular regulatory feature to instead facilitate translation of multiple proteins from a single mRNA.

The 5′ untranslated region (UTR) of the ORF35-37 mRNA contains two uORFs (uORF1 and uORF2), with uORF2 playing a more dominant role in translational regulation of this locus (7). uORF2 overlaps with the start codon of the 5′ ORF35 gene, and thus its translation causes ribosomes to bypass ORF35 and instead reinitiate downstream at the ORF36 start site (Fig. 1B) (7). A single point mutation disrupting uORF2 in the KSHV genome dramatically impairs ORF36 expression during infection, confirming the importance of uORF-assisted ribosome scanning in regulating translation of this polycistronic mRNA (7). To determine the extent to which the disruption of uORF2 impacts KSHV replication, we compared the production of progeny virions from cells infected with KSHV derived from the BAC16 recombineering system containing the uORF2 mutation (BAC16-Δ2; ATG→TTG) to that of a revertant mutant rescue virus in which the mutation had been repaired (BAC16-Δ2-MR; TTG→ATG) (Fig. 1A). We previously confirmed that the two cell lines express similar levels of the viral latency antigen LANA and reactivate with equal levels of efficiency (7). Upon lytic reactivation of iSLK-PURO cells harbor-

ing BAC16-Δ2 and BAC16-Δ2-MR for 48 h, cell-free supernatants were transferred to recipient 293A cells. BAC16 contains a green fluorescent protein (GFP) marker enabling direct visualization of infected cells by fluorescence microscopy (Fig. 1D) or quantitation by flow cytometry (Fig. 1E). In both cases, there was a dramatic reduction in the level of infectious virus produced from the uORF2 mutant, calculated to be 36.65-fold ± 0.11-fold by flow cytometry (Fig. 1E). Thus, uORF2-directed translation of ORF36 plays a key role in viral replication.

Given the importance of this locus in the KSHV life cycle, we sought to define in more detail the factors governing its unusual translational regulation. Although we had previously demonstrated translation of the upstream ORF35 gene in transient-transfection experiments, this protein is of unknown function and its expression has not been confirmed during infection. Thus, to verify that ORF35 is expressed during lytic replication, we engineered an in-frame FLAG-epitope tag within the coding region of ORF35 at nucleotide (nt) position 55796 in KSHV BAC16 (BAC16-WT-iFLAG; Fig. 2A) (12). An internal tag was chosen because insertion of an N- or C-terminal tag would disrupt either the coding region of uORF2 or the N terminus of ORF36, respectively. BAC16-WT-iFLAG was stably transfected into iSLK-PURO cells bearing a doxycycline-inducible replication and transcription activator (RTA) expression system to enable lytic reactivation, as described previously (7, 12, 13). Immunoblot analysis using polyclonal antisera specific for FLAG or ORF36 revealed that both proteins were readily detectable at 96 h post-lytic reactivation, confirming that the ORF35-37 transcript is functionally dicistronic during KSHV infection (Fig. 2B).

An interesting feature of the translational regulation of this locus is the apparent disparity between the relative levels of effi-
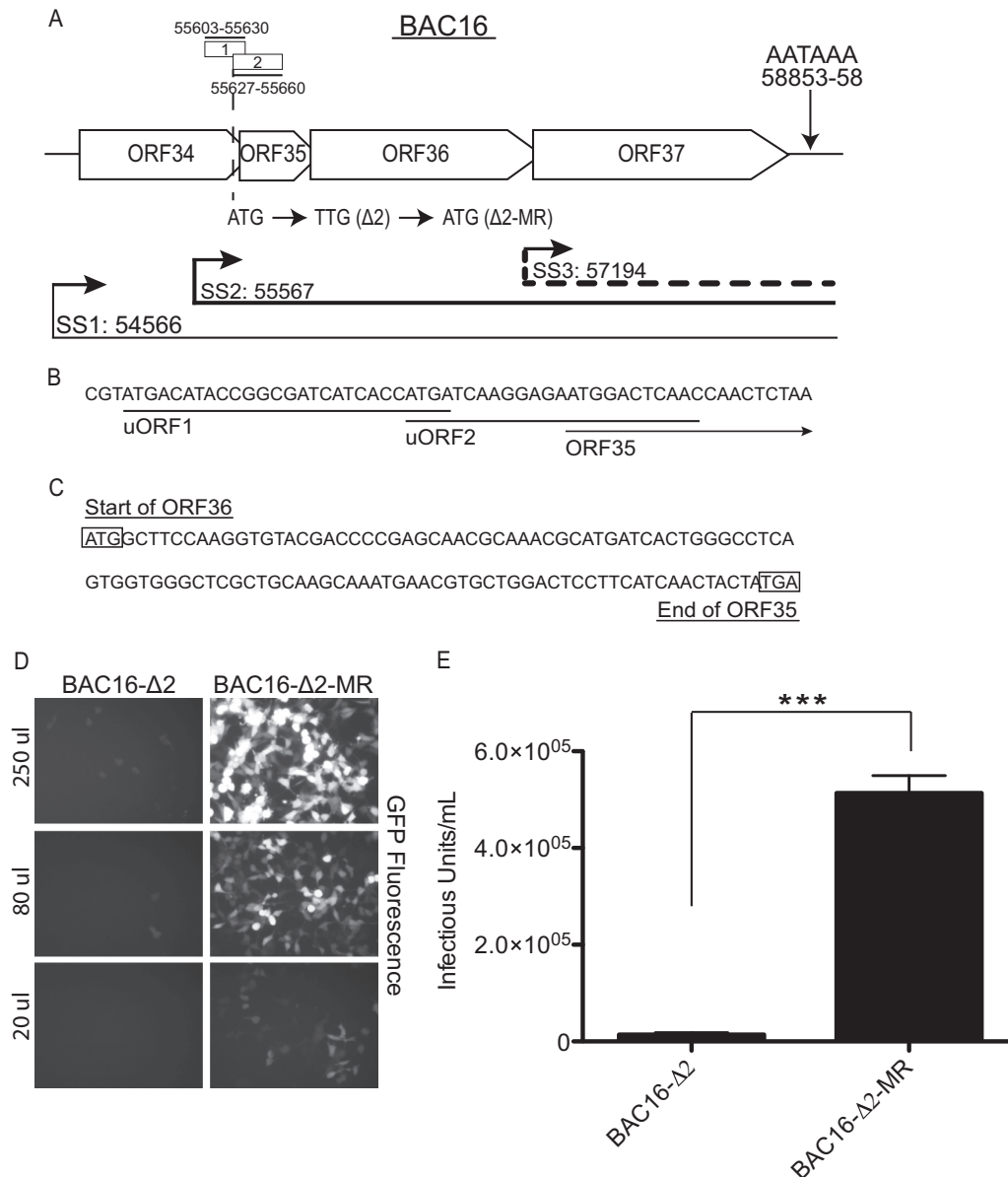
FIG 1 Disruption of uORF2 leads to a defect in the production of infectious viral particles. (A) A schematic presentation of the *ORF34-37* genetic locus showing the ORF34-37, ORF35-37, and ORF37 mRNAs with thin, thick, and dashed lines, respectively. Start sites (SS) for each transcript and uORF1 and uORF2 genomic location are indicated according to the nucleotide position described by Russo et al. (30). The single poly(A) signal used by all four ORFs for transcription termination is shown. The nucleotide mutated to generate the uORF2 start codon mutant (ATG → TTG; Δ2) and the repaired marker rescue (TTG→ATG; Δ2-MR) is indicated. (B) Start and coding sequences for uORF1 and uORF2 and the N terminus of ORF35. (C) The region of overlap of sequence between ORF35 and ORF36. The ORF36 start codon and the ORF35 stop codon are boxed. (D and E) 293A cells (2×10^5 per well) were seeded 12 h prior to infection. At 48 h post-lytic reactivation with doxycycline, cell-free virus supernatant was harvested from the iSLK-PURO BAC16-Δ2 cell line or the Δ2-MR cell line, and then various dilutions were used to inoculate 293A cells via spinfection ($2,000 \times g$ for 45 min at 30°C). The cells were then incubated for 1 h, the inoculum was replaced with fresh media, and infection was allowed to proceed for 24 h prior to visualization by fluorescence microscopy (D) or analysis by flow cytometry (E). The percentage of GFP-positive 293A cells was detected using a FACSCanto II cell analyzer (BD Bioscience, San Jose, CA). Infectious unit (IU) values represent the number of GFP-positive cells in each well at the time of analysis. The experiment was performed in triplicate; error bars represent the standard deviations of the results of comparisons between replicates. Statistical significance was evaluated with a two-tailed unpaired *t* test (***, $P < 0.0001$).

ciency of initiation at the upstream ORF35 gene versus the downstream ORF36 gene on the polycistronic mRNA. Protein accumulation is dependent on both the initiation rate of the ORF35 and ORF36 start codons and the half-life of each protein. ORF35 and ORF36 proteins have different half-lives (Fig. 2C and D), so, to limit this complication, reporter constructs were generated with

the ORF35 or ORF36 coding region replaced with the *Renilla* luciferase gene, thus allowing initiation at each ORF (AUG_{ORF35} and AUG_{ORF36}) to be monitored separately but from the authentic upstream sequence context. It should be noted, however, that even the *Renilla* replacement does not completely eliminate the half-life disparity, as the seven amino acids derived from ORF35
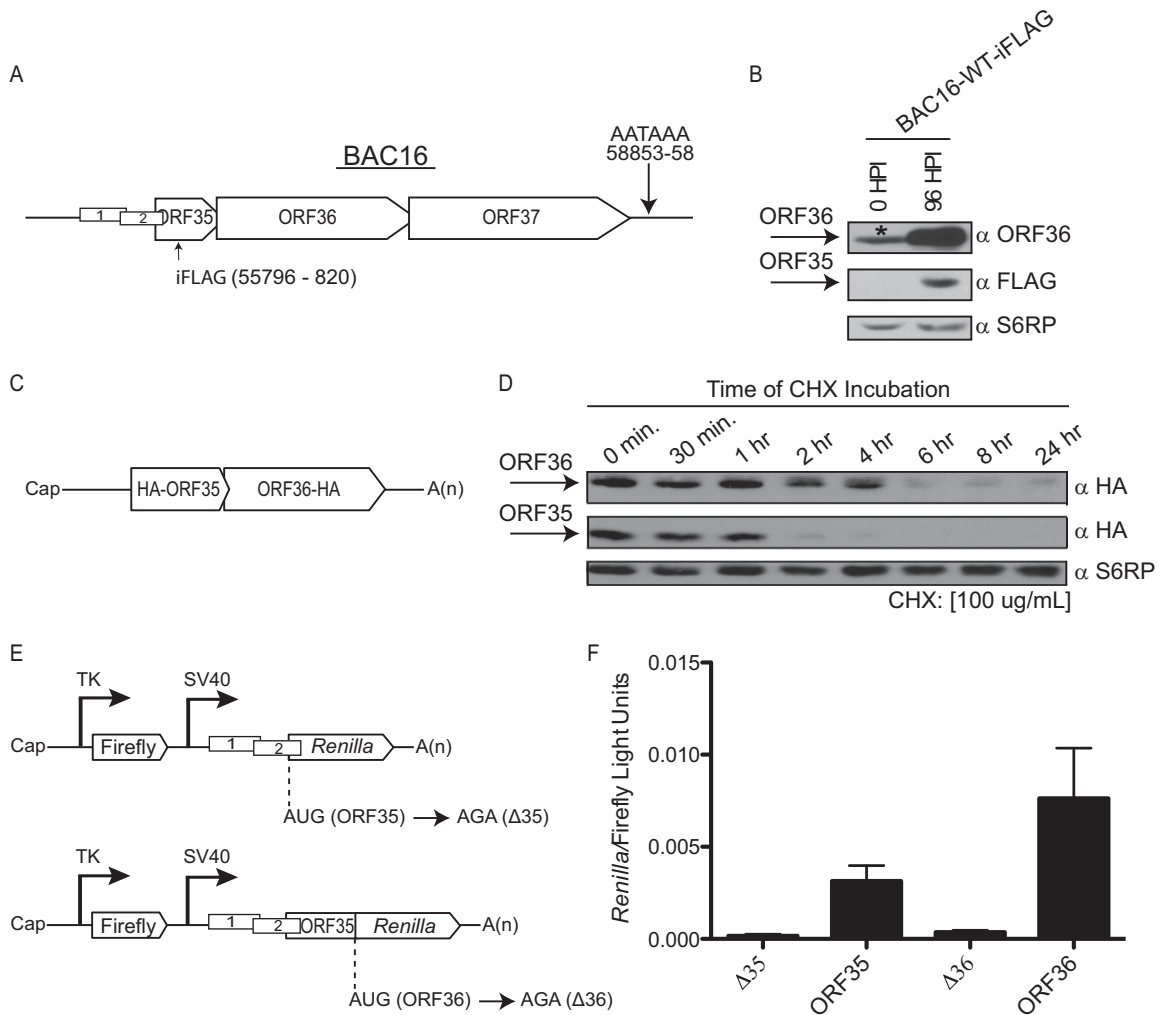
FIG 2 Analysis of the ratio of ORF35 expression to ORF36 expression during infection and transfection. (A) A schematic presentation of the ORF35-37 mRNA and the single poly(A) signal used by all four ORFs for transcription termination is shown. The position of the internal FLAG epitope tag (iFLAG) within ORF35 is indicated. (B) iSLK-PURO cells stably harboring the KSHV BAC16-iFLAG were either left untreated or lytically reactivated for 96 h. Protein lysates were subjected to Western blotting with antibodies against ORF36, FLAG-tagged ORF35, or the ribosomal protein S6RP (as a loading control). The asterisk (*) denotes a cross-reactive protein that comigrates with ORF36 in uninduced iSLK-PURO cells. HPI, hours postinfection; WT, wild type. (C) Schematic of the 5′ UTR hemagglutinin (HA)-ORF35-ORF36-HA plasmid, constructed as described in reference 7. (D) 293T cells were transfected with the 5′ UTR HA-ORF35-ORF36-HA construct. After 24 h, the cells were treated with 100 μg/ml of the translation elongation inhibitor cycloheximide (CHX), whereupon protein lysates were harvested at the indicated time points and immunoblotted with anti-HA antibodies or S6RP (as a loading control). (E) Schematic of the psiCHECK-2 (Invitrogen) dual-luciferase constructs that harbor firefly and *Renilla* luciferase under the independent control of the thymidine kinase (TK) and simian virus 40 (SV40) promoters, respectively. For the ORF35 construct, upstream of *Renilla* is the native 72-nucleotide (nt) 5′ UTR of the ORF35-37 mRNA containing uORF1 and uORF2 and the first 21 nt of ORF35. The *Renilla* AUG was mutated to AGA, causing its translation to initiate from the native ORF35 start codon and thus serve as a readout for ORF35 translation initiation. The ORF36 construct harbors the native 5′ UTR of the ORF35-37 mRNA, the uORF1 and uORF2 regulatory elements, and the first 352 nt of ORF35 followed by *Renilla* luciferase, which serves as a reporter for ORF36 translation initiation. The nucleotides mutated to disrupt AUG$_{ORF35}$ (Δ35) and AUG$_{ORF36}$ (Δ36) are shown. (F) The indicated constructs were transfected into 293T cells, and a dual-luciferase assay was performed 24 h posttransfection to determine the relative levels of *Renilla* luciferase activity and firefly luciferase activity. The experiment was performed in triplicate; error bars represent the standard deviations of the results of comparisons between replicates.

that must be present on the N terminus of *Renilla* to preserve the uORF2 context moderately destabilize the reporter protein by ~1.4-fold (data not shown). This plasmid backbone also harbors a firefly luciferase under the control of an independent promoter to provide an internal control of transfection efficiency (Fig. 2E). The ratio of *Renilla* luciferase to firefly luciferase from each construct indicated that the ratio of translation initiation at AUG$_{ORF35}$ to that at AUG$_{ORF36}$ is 0.4128 ± 0.028:1.0 (Fig. 2F), which is likely a modest underrepresentation of ribosome engage-

ment at ORF35 due to the nonidentical levels of stability of *Renilla* between the two constructs. Thus, in addition to being dicistronic, translation from the KSHV ORF35-37 transcript is unusual in that initiation at ORF36 occurs at least as frequently as initiation at the 5′ ORF35 cistron, despite the AUG$_{ORF35}$ being flanked by a strong Kozak consensus sequence.

It was previously shown that uORF2 exerted a far greater impact on translation of ORF35 and ORF36 than uORF1 when each uORF was mutated individually (7). However, both uORFs are
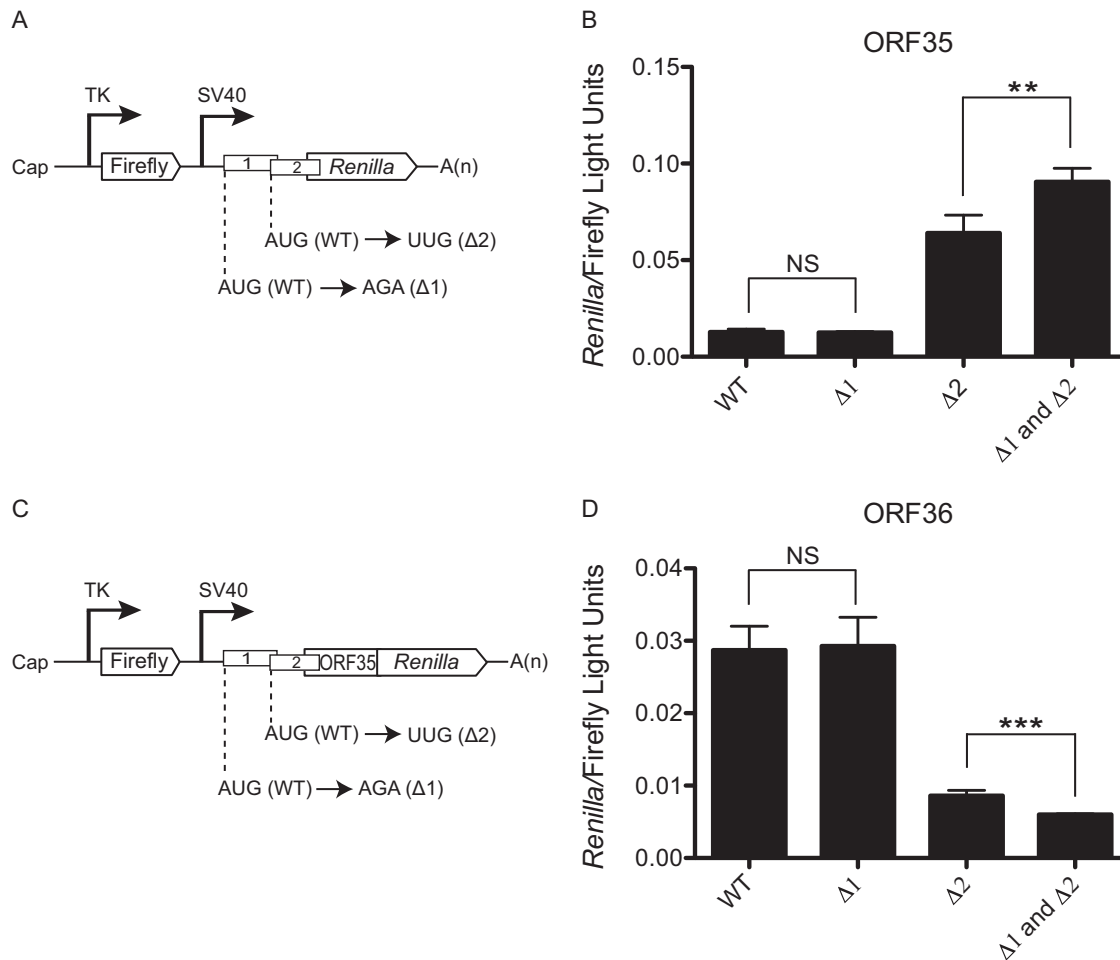
FIG 3 uORF1 and uORF2 govern expression of ORF35 and ORF36. (A and B) Schematics of the ORF35 (A) and ORF36 (C) reporter dual-luciferase constructs. The nucleotides mutated to disrupt AUG_{uORF1} (Δ1) and AUG_{uORF2} (Δ2) are shown. (B and D) The indicated constructs were transfected into 293T cells, and a dual-luciferase assay was performed 24 h posttransfection to determine the relative levels of firefly luciferase activity and *Renilla* luciferase activity. The experiment was performed in triplicate; error bars represent the standard deviations of the results of comparisons between replicates. Statistical significance was evaluated with a two-tailed unpaired *t* test (NS, $P > 0.05$; **, $P < 0.001$; ***, $P < 0.0001$).

positionally conserved in a number of related viruses, suggesting that uORF1 may nonetheless play an important regulatory role (7). We therefore examined how individual versus combined mutations of uORF1 and uORF2 influenced translation of the ORF35-37 polycistronic mRNA in the context of the *Renilla* luciferase constructs described above (Fig. 3A and C). In agreement with previous results, disruption of uORF2 alone (Δ2) led to increased ORF35 translation and compromised expression of ORF36, whereas disruption of AUG_{uORF1} alone (Δ1) had no significant effect (Fig. 3B and D). However, the combined disruptions of both AUG_{uORF1} (Δ1) and AUG_{uORF2} (Δ2) led to a moderate and yet reproducible increase in ORF35 expression and decrease in ORF36 expression (Fig. 3B and D). These data suggest that when AUG_{uORF1} is disrupted, ribosomes continue to scan and alternatively initiate at AUG_{uORF2}, with a similar net result of ORF35 repression and reinitiation at ORF36 (Fig. 3B and D, lane 1 versus lane 2). When both uORFs are disrupted, however, the ribosomes that would have been captured by AUG_{uORF2} now initiate at AUG_{ORF35} and are thus precluded from reinitiating at ORF36. This would lead to an additional increase in ORF35 ex-

pression and a corresponding drop in ORF36 levels. We conclude that uORF1 and uORF2 are both repressive elements of ORF35.

Our data indicate that the majority of ribosomes that translate uORF1 do not reinitiate at AUG_{ORF35}, likely due to the inadequate intercistronic distance (9 nt) between AUG_{uORF1} and AUG_{ORF35}, although it remains formally possible that a small fraction of ribosomes may be capable of reinitiating at the ORF35 start codon (8, 14, 15). Thus, why does ORF35 expression persist despite the presence of two upstream repressive elements? The most likely possibility is that translational engagement at AUG_{ORF35} occurs by ribosomes that have scanned in a leaky manner past both AUG_{uORF1} and AUG_{uORF2}. If this were occurring, then enhancing the Kozak consensus sequence surrounding uORF1 and uORF2 start codons should restrict leaky scanning and dampen ORF35 expression. To test this hypothesis, the -3, -2, -1, and $+4$ unfavorable Kozak consensus sequence flanking AUG_{uORF1} was mutated to the preferred context (CguAUGA → AccAUGG; KCS1 enh) and the intermediate context flanking AUG_{uORF2} was enhanced at the -4 position from A to G (AccAUGA → AccAUGG; KCS2 enh) (Fig. 4A and C) (16, 17). Indeed, enhancing the
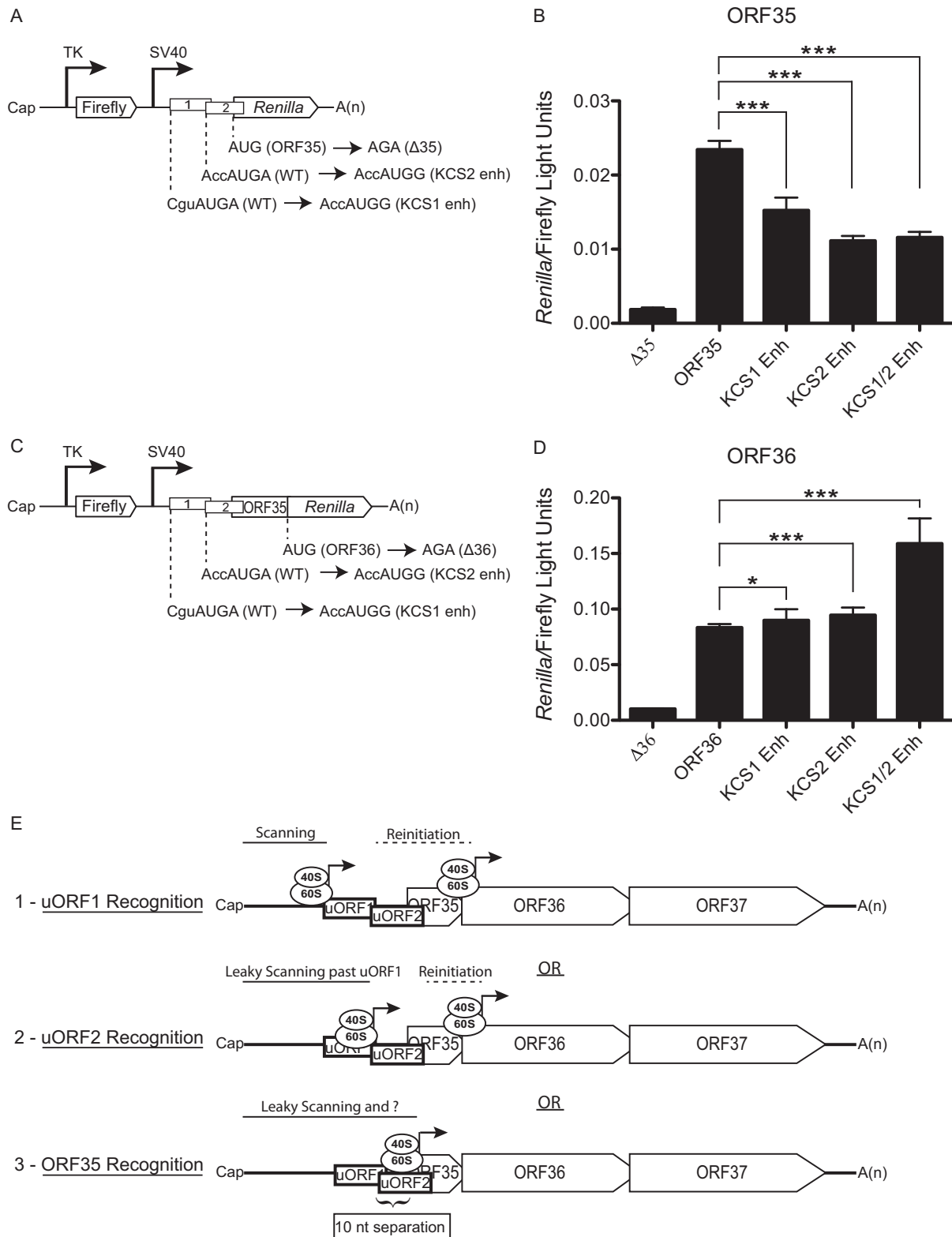
FIG 4 Leaky scanning past AUG_{uORF1} and AUG_{uORF2} facilitates ORF35 expression. (A and C) Diagram indicating the nucleotide mutations used to enhance the Kozak consensus sequence of the uORF1 (KCS1 enh) and/or the uORF2 (KCS2 enh) start codons within the ORF35 (A) and ORF36 (C) dual-luciferase reporter constructs. (B and D) The indicated constructs were transfected into 293T cells, and a dual-luciferase assay was performed 24 h posttransfection to determine the relative levels of firefly luciferase activity and *Renilla* luciferase activity. The experiment was performed in triplicate; error bars represent the standard deviations of the results of comparisons between replicates. Statistical significance was evaluated with a two-tailed unpaired t test (*, $P < 0.05$; **, $P < 0.001$; ***, $P < 0.0001$). (E) A model of the three translational programs governing expression from the ORF35-37 polycistronic mRNA. (1) Scanning ribosomes initiate translation at uORF1, terminate translation, continue to scan, and then reinitiate translation downstream of the ORF35 start codon. (2) Scanning ribosomes scan in a leaky manner past AUG_{uORF1} and initiate translation at AUG_{uORF2}, terminate translation, continue to scan, and then reinitiate translation at the AUG_{ORF36}. (3) Scanning ribosomes scan in a leaky manner past AUG_{uORF1} and AUG_{uORF2} to initiate translation at AUG_{ORF35}. The 10-nt separation between AUG_{uORF2} and AUG_{ORF35} is depicted.

AUG$_{uORF1}$ and AUG$_{uORF2}$ contexts either independently or in combination led to a repression of ORF35 (Fig. 4B). These data are consistent with the preinitiation complex initiating with higher fidelity at AUG$_{uORF1}$ and AUG$_{uORF2}$, allowing fewer ribosomes to scan past the uORFs in favor of AUG$_{ORF35}$. In agreement with this model, both the KCS1 and KCS2 mutants led to an increase in ORF36 expression, which requires AUG$_{ORF35}$ to be bypassed (Fig. 4D). Thus, leaky scanning past uORF1 and uORF2 facilitates translation of ORF35, while a termination-reinitiation mechanism after both uORF1 and uORF2 enables translation of the downstream ORF36 gene (Fig. 4E). This mechanism results in fairly balanced initiation rates for both proteins, though ORF36 accumulates to higher levels due to its increased protein stability.

It is notable that ORF35 protein expression persisted at 40% even in the face of two upstream AUGs that both engage the translation apparatus (Fig. 4B) (7). This suggests that an additional mechanism may facilitate ribosomal recognition of the AUG$_{ORF35}$ to ensure a baseline expression of this protein. It has been postulated that the close apposition of two AUGs ($\leq$15 nt) may modify leaky scanning such that initiation is no longer strictly sequential with 5′-to-3′ polarity but is competitive (18, 19). In this regard, the close proximity of the uORF2 and ORF35 start codons (10 nt) may be important for the dicistronic character of this mRNA (Fig. 4E) (18, 20, 21). Finally, while this is a rare example of a uORF enabling viral polycistronic translation, it is possible that a similar mechanism may regulate a subset of the $\geq$4,000 human mRNAs containing uORFs that overlap a primary ORF (8, 22–26). Engagement of uORFs in this manner could therefore expand the coding capacity of the transcriptome, as has been documented for C/EBPα and C/EBPβ protein isoforms and the innate mitochondrial antiviral signaling (MAVS) immune regulator (27–29).

ACKNOWLEDGMENTS

REFERENCES

1. **Kedes DH, Ganem D.** 1997. Sensitivity of Kaposi's sarcoma-associated herpesvirus replication to antiviral drugs. Implications for potential therapy. J. Clin. Invest. **99:**2082–2086.
2. **Casper C, Krantz EM, Corey L, Kuntz SR, Wang J, Selke S, Hamilton S, Huang ML, Wald A.** 2008. Valganciclovir for suppression of human herpesvirus-8 replication: a randomized, double-blind, placebo-controlled, crossover trial. J. Infect. Dis. **198:**23–30. http://dx.doi.org/10.1086/588820.
3. **Cannon JS, Hamzeh F, Moore S, Nicholas J, Ambinder RF.** 1999. Human herpesvirus 8-encoded thymidine kinase and phosphotransferase homologues confer sensitivity to ganciclovir. J. Virol. **73:**4786–4793.
4. **Martin DF, Kuppermann BD, Wolitz RA, Palestine AG, Li H, Robinson CA.** 1999. Oral ganciclovir for patients with cytomegalovirus retinitis treated with a ganciclovir implant. Roche Ganciclovir Study Group. N. Engl. J. Med. **340:**1063–1070.
5. **Bieleski L, Talbot SJ.** 2001. Kaposi's sarcoma-associated herpesvirus vCyclin open reading frame contains an internal ribosome entry site. J. Virol. **75:**1864–1869. http://dx.doi.org/10.1128/JVI.75.4.1864-1869.2001.
6. **Grundhoff A, Ganem D.** 2001. Mechanisms governing expression of the v-FLIP gene of Kaposi's sarcoma-associated herpesvirus. J. Virol. **75:** 1857–1863. http://dx.doi.org/10.1128/JVI.75.4.1857-1863.2001.
7. **Kronstad LM, Brulois KF, Jung JU, Glaunsinger BA.** 2013. Dual short upstream open reading frames control translation of a herpesviral polycistronic mRNA. PLoS Pathog. **9:**e1003156. http://dx.doi.org/10.1371/journal.ppat.1003156.
8. **Calvo SE, Pagliarini DJ, Mootha VK.** 2009. Upstream open reading frames cause widespread reduction of protein expression and are polymorphic among humans. Proc. Natl. Acad. Sci. U. S. A. **106:**7507–7512. http://dx.doi.org/10.1073/pnas.0810916106.
9. **Cao J, Geballe AP.** 1995. Translational inhibition by a human cytomegalovirus upstream open reading frame despite inefficient utilization of its AUG codon. J. Virol. **69:**1030–1036.
10. **Shabman RS, Hoenen T, Groseth A, Jabado O, Binning JM, Amarasinghe GK, Feldmann H, Basler CF.** 2013. An upstream open reading frame modulates ebola virus polymerase translation and virus replication. PLoS Pathog. **9:**e1003147. http://dx.doi.org/10.1371/journal.ppat.1003147.
11. **Wu HY, Guan BJ, Su YP, Fan YH, Brian DA.** 2014. Reselection of a genomic upstream open reading frame in mouse hepatitis coronavirus 5′-untranslated-region mutants. J. Virol. **88:**846–858. http://dx.doi.org/10.1128/JVI.02831-13.
12. **Brulois KF, Chang H, Lee AS, Ensser A, Wong LY, Toth Z, Lee SH, Lee HR, Myoung J, Ganem D, Oh TK, Kim JF, Gao SJ, Jung JU.** 27 June 2012. Construction and manipulation of a new Kaposi's sarcoma-associated herpesvirus bacterial artificial chromosome clone. J. Virol. http://dx.doi.org/10.1128/JVI.01019-12.
13. **Myoung J, Ganem D.** 2011. Generation of a doxycycline-inducible KSHV producer cell line of endothelial origin: maintenance of tight latency with efficient reactivation upon induction. J. Virol. Methods **174:**12–21. http://dx.doi.org/10.1016/j.jviromet.2011.03.012.
14. **Kozak M.** 1987. Effects of intercistronic length on the efficiency of reinitiation by eucaryotic ribosomes. Mol. Cell. Biol. **7:**3438–3445.
15. **Grant CM, Hinnebusch AG.** 1994. Effect of sequence context at stop codons on efficiency of reinitiation in GCN4 translational control. Mol. Cell. Biol. **14:**606–618.
16. **Kozak M.** 1997. Recognition of AUG and alternative initiator codons is augmented by G in position +4 but is not generally affected by the nucleotides in positions +5 and +6. EMBO J. **16:**2482–2492. http://dx.doi.org/10.1093/emboj/16.9.2482.
17. **Kozak M.** 1986. Point mutations define a sequence flanking the AUG initiator codon that modulates translation by eukaryotic ribosomes. Cell **44:**283–292. http://dx.doi.org/10.1016/0092-8674(86)90762-2.
18. **Matsuda D, Dreher TW.** 2006. Close spacing of AUG initiation codons confers dicistronic character on a eukaryotic mRNA. RNA **12:**1338–1349. http://dx.doi.org/10.1261/rna.67906.
19. **McFadden N, Bailey D, Carrara G, Benson A, Chaudhry Y, Shortland A, Heeney J, Yarovinsky F, Simmonds P, Macdonald A, Goodfellow I.** 2011. Norovirus regulation of the innate immune response and apoptosis occurs via the product of the alternative open reading frame 4. PLoS Pathog. **7:**e1002413. http://dx.doi.org/10.1371/journal.ppat.1002413.
20. **Kozak M.** 1995. Adherence to the first-AUG rule when a second AUG codon follows closely upon the first. Proc. Natl. Acad. Sci. U. S. A. **92:** 2662–2666. http://dx.doi.org/10.1073/pnas.92.7.2662.
21. **Williams MA, Lamb RA.** 1989. Effect of mutations and deletions in a bicistronic mRNA on the synthesis of influenza B virus NB and NA glycoproteins. J. Virol. **63:**28–35.
22. **Chen A, Kao YF, Brown CM.** 2005. Translation of the first upstream ORF in the hepatitis B virus pregenomic RNA modulates translation at the core and polymerase initiation codons. Nucleic Acids Res. **33:**1169–1181. http://dx.doi.org/10.1093/nar/gki251.
23. **Cao F, Tavis JE.** 2011. RNA elements directing translation of the duck hepatitis B virus polymerase via ribosomal shunting. J. Virol. **85:**6343–6352.
24. **Dominguez DI, Ryabova LA, Pooggin MM, Schmidt-Puchta W, Fütterer J, Hohn T.** 1998. Ribosome shunting in cauliflower mosaic virus. Identification of an essential and sufficient structural element. J. Biol. Chem. **273:**3669–3678.
25. **Fütterer J, Hohn T.** 1991. Translation of a polycistronic mRNA in the presence of the cauliflower mosaic virus transactivator protein. EMBO J. **10:**3887–3896.

26. **Fütterer J, Kiss-Laszlo Z, Hohn T.** 1993. Nonlinear ribosome migration on cauliflower mosaic virus 35S RNA. Cell **73:**789–802. http://dx.doi.org/10.1016/0092-8674(93)90257-Q.

27. **Calkhoven CF, Muller C, Leutz A.** 2000. Translational control of C/EBPalpha and C/EBPbeta isoform expression. Genes Dev. **14:**1920–1932.

28. **Wethmar K, Smink JJ, Leutz A.** 2010. Upstream open reading frames: molecular switches in (patho)physiology. Bioessays **32:**885–893.

29. **Brubaker SW, GA, Mills EW, Ingolia NT, Kagan JC.** 2014. A bicistronic MAVS transcript highlights a class of truncated variants in antiviral immunity. Cell **156:**800–811. http://dx.doi.org/10.1016/j.cell.2014.01.021.

30. **Russo JJ, Bohenzky RA, Chien MC, Chen J, Yan M, Maddalena D, Parry JP, Peruzzi D, Edelman IS, Chang Y, Moore PS.** 1996. Nucleotide sequence of the Kaposi sarcoma-associated herpesvirus (HHV8). Proc. Natl. Acad. Sci. U. S. A. **93:**14862–14867. http://dx.doi.org/10.1073/pnas.93.25.14862.